Final Report: NAG5-10613, "High-Sensitivity Optical Techniques for Atmospheric Spectroscopy, Kinetics and Remote Sensing"

A principal objective of the work supported by this Grant has been to use IntraCavity Laser Absorption Spectroscopy (ICLAS) to acquire data on weakly absorbing species of atmospheric interest that are not accessible, or cannot be determined with sufficient precision, using conventional spectroscopic instrumentation. The principal focus has been to adapt the existing instrument to carry out Kinetic studies using IntraCavity Absorption Spectroscopy (KICAS) in order to measure rate parameters for weakly absorbing, environmentally significant species. Additional related work has been carried out in collaboration with Prof. M.J. Molina's program on air pollution in the Mexico City Metropolitan Area on modeling the role of these species in atmospheric chemistry.

1.   Kinetic Measurements by IntraCavity Absorption Spectroscopy

Nitrosyl hydride, HNO, is an important intermediate in a variety of oxidation processes in the formation of NO_x during combustion. Elementary reactions involving HNO are also of interest in understanding the removal and formation of nitrogen oxides and ammonia in the atmosphere. The kinetics of HNO reactions in the presence of O_2 have been measured in an ICLAS experiment using flash photolysis of ammonia in the presence of oxygen[1]. We combined Intracavity Laser Absorption Spectroscopy (ICLAS) with discharge flow kinetics in order to verify previously reported rate constants and validate and/or calibrate our method, which we have termed Kinetic studies using IntraCavity Absorption Spectroscopy (KICAS).

Intracavity Laser Absorption Spectroscopy (ICLAS) is a powerful method to improve both spectroscopic and kinetic parameters for trace atmospheric species (weak absorbers, free radicals, etc.). ICLAS is a high-resolution, high-sensitivity spectroscopic technique. Effective path lengths that can vary between a few km to over 100 km, leading to extremely high absorption sensitivity, provide the sensitivity for the technique. High signal/noise is provided via spectral averaging and time-correlated double sampling (where applicable). We modified the ICLAS system to enable kinetic measurements of transient and reactive species in a flow tube. Both cavity ring-down spectroscopy and chemiluminescence have been used to measure reactions in which the concentration of the species of interest was dependent on distance or time[2][3][4]. Our measurements, reported below, show that ICLAS may be employed for this purpose.

Experimental – ICLAS. The experimental apparatus was similar to that used for previous spectroscopic measurements on the oxygen *A*-bands [Publication No. 7] and *trans*-HONO [Publication No. 10]. Pump radiation from an argon ion laser was focused on a Ti:sapphire crystal which acts as a homogeneously broadened gain medium. An acousto-optic modulator (AOM) interrupts the pump laser beam to initiate a long pulse of radiation. The signal is sent to a spectrograph/CCD detector, after an adjustable delay provided by a second AOM. This adjustable delay is the generation time, t_g, which is directly related to the effective absorption path length by

[1] M.G. Bryukov, A.A. Kachanov, R. Timonnen, J. Seetula, J. Vandoren, and O.M. Sarkisov, *Chem. Phys. Letts.* **208**, 392 (1993).
[2] Lee, SY *et al.*, *Chem. Phys. Letts.*, **257**, 415 (1996).
[3] Yi, HJ; Jee, YJ; Lee, KW; Jung, KJ. *Chem. Phys. Letts*, **327**, 325 (2000).
[4] Brown, SS; Ravishankara, AR; Stark, H. *J. Phys. Chem.*, **104**, 7044 (2000)

$$L_{eff} = c\ t_g\ (l/L), \tag{1}$$

where l is the length of the sampling region within the cavity, and L is the total length of the optical cavity.

To carry out kinetic measurements, a flow cell replaces the static cell in the laser cavity. We have employed both an *axial measurement* approach, in which the flow is along the axis of detection and a *transverse measurement* approach, in which the flow is transverse to the axis of detection. The transverse measurement technique gave the more reliable results, and is reported here.

HNO was produced by reaction of H atoms with NO in a nitrogen stream. Hydrogen atoms were generated by passing helium gas containing a small amount of hydrogen through a microwave discharge upstream. Detection of HNO was carried out via the $\tilde{A}^1A'' \leftarrow \tilde{X}^1A'$ electronic transition near 760 nm. A portion of the HNO spectrum is shown in Figure 1. The spectra were frequency calibrated to within 0.01 cm^{-1} using known oxygen lines. Because ICLAS adheres to Beer's Law, the integrated absorbance of the $^RQ_0(8)$ transition was used to monitor reaction progress. Based on the absorption cross-section of the $^RR_3(6)$ transition of HNO measured by Cheskis et al.[5] and using Franck-Condon factors from Mordaunt et al.[6] and rotational line strength factors calculated using expressions derived by Lide[7], the absorption cross-section of the $^RQ_0(8)$ transition of the (000) ← (000) band of HNO was calculated to be 4.25 x 10^{-17} cm^2 molecule^{-1}.
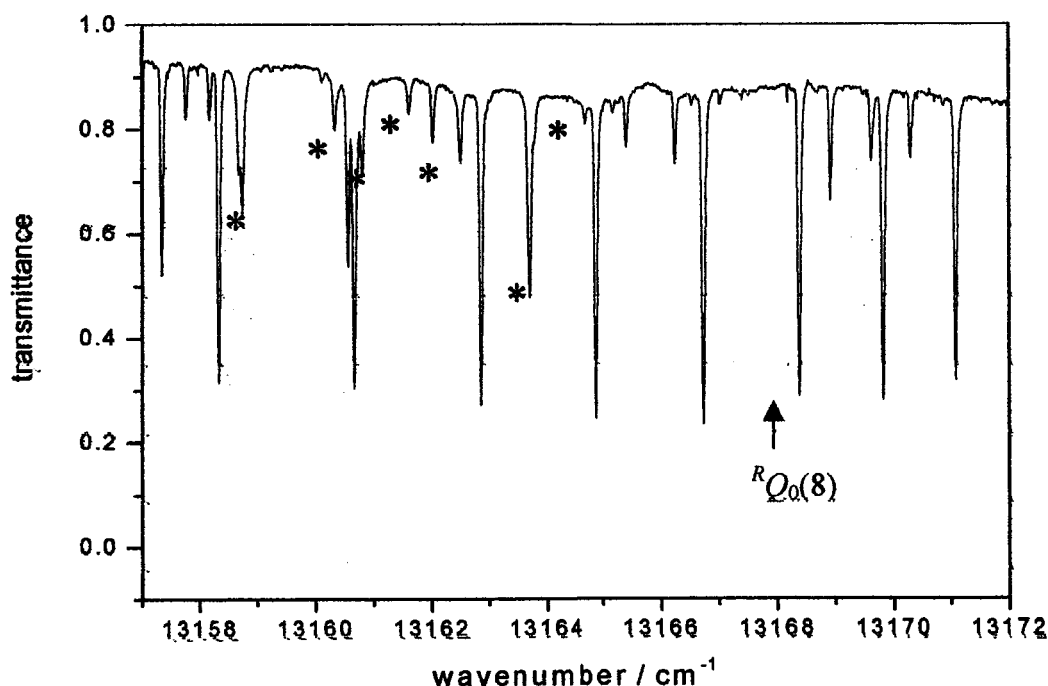

Figure 1. Experimental spectrum of the high J lines of the $K_a'' = 0$ subband of the Q branch. Transitions labeled with an asterisk are due to atmospheric oxygen absorption, used in frequency calibrating spectra.

[5] Cheskis, SG; Nadtochenko, VA; Sarkisov, OM. *Int. J. Chem. Kinet.*, **13**, 1041 (1981).
[6] Mordaunt, DH, et al.. *J. Chem. Phys.*, **107**, 6603 (1997).
[7] Lide, DR. *J. Chem. Phys.*, **20**, 1761, (1952).

3

The transverse measurement setup is shown below in Figure 2. All measurements were performed at a generation time of 70 μs with a traveling-wave, ring configuration of the ICLAS laser. The occupation ratio and effective path length of this set-up are 1.54% and 323 m, respectively. The flow tube used is made of Pyrex and has an inner diameter of 1.63 cm. The generation scheme is similar to the previously described one, with the only major difference being the injector.

Due to geometrical constraints associated with our optical bench and the ICLAS laser setup, we are left with 'sidearms' in the design of the flow cell, marked X and Y in Figure 2. Significant diffusion into these regions would limit the system's capabilities to accurately measure HNO formation kinetics and reaction kinetics. However, the introduction of a 'gas-curtain' can effectively contain the HNO to the desired mixing region via a counter-flow and maintain the flow products/reactants perpendicular to the detection axis. Also, the increased pressure in the reactor is beneficial for a faster formation of HNO. The gas curtain is simply an introduction of helium at ports 1 and 2, as shown in Figure 2.
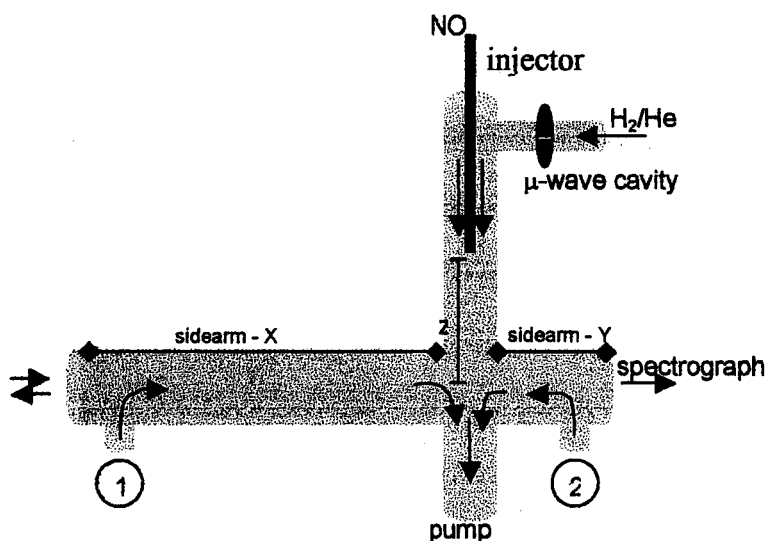

Figure 2. Schematic of experimental apparatus for transverse measurements using an ICLAS laser.

As shown in Figure 3, it is clear that with the introduction of the gas curtain at pressures ≥ 0.5 Torr, the diffusion of the radical to the 'sidearms' is sufficiently limited, and the observed HNO is a measure of radical formation kinetics.
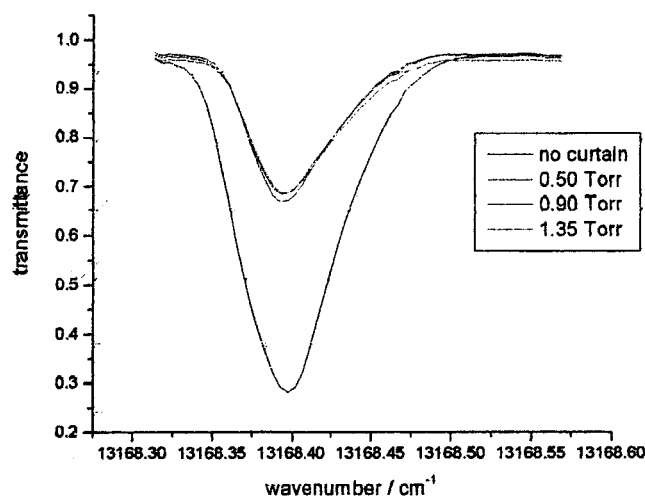
4

Figure 3. Demonstration of 'gas-curtain' efficacy at different concentrations of helium introduced at ports 1 and 2. The numbers in the legend are a measure of the flow/concentration of helium introduced at *each* port. Increased flow rates do not indicate a decrease in the transmittance of the HNO signal.

Due to the potential dependence of the discharge efficiency on the system's total pressure, it is also necessary to determine an appropriate operating range of pressures, such that we are certain that any change in the HNO concentration is due to kinetic processes, and not a function of the discharge. The results for measurements made over a range of pressures for a system with helium carrier gas are shown in Figure 4. It is clear from Figure 4 that our discharge is stable over a sufficiently broad pressure range to conduct kinetic measurements.
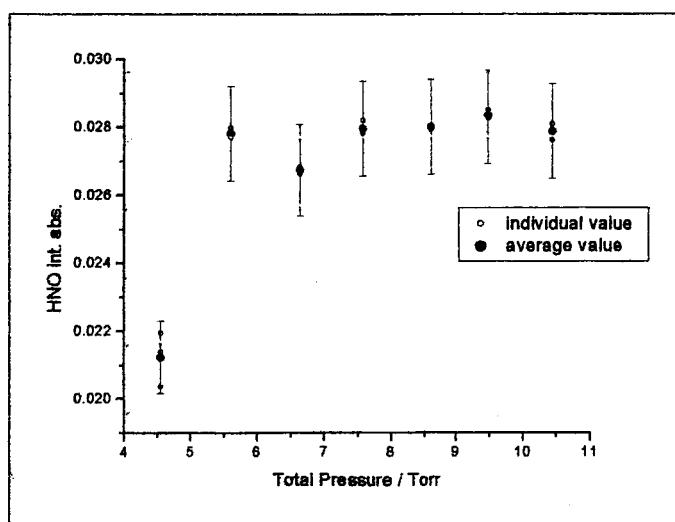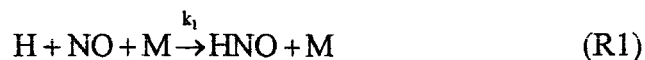

Figure 4. Microwave discharge efficiency measured as a function of HNO concentration over a range of pressures. It is apparent that the current reactor operates in a consistent fashion in the 5-11 Torr range.

5

Experimental results. The following reactions are relevant to the study of HNO formation using ICLAS as the detection method:

$$H + NO + M \xrightarrow{k_1} HNO + M \qquad (R1)$$

$$H + H + M \xrightarrow{k_2} H_2 + M \qquad (R2)$$

$$HNO + H \xrightarrow{k_3} H_2 + NO \qquad (R3)$$

$$HNO + wall \xrightarrow{k_w} decay \qquad (R4)$$

The procedure used for determining the rate of reaction (R1) with this method is similar to that commonly used for low-pressure flow tubes; however, the product, rather than reacting species, is monitored. Nitric oxide and helium were injected at a fixed rate, and their number densities were calculated assuming complete mixing in the region downstream of the injector. In each reaction, both NO and He (carrier gas = M) were present in several orders of magnitude greater than the estimated hydrogen atom concentration, creating pseudo-first-order conditions. The plasma discharge was initiated or 'lit' and the position of the moveable injector was varied to generate a series of kinetic curves. A non-linear least squares fit was then performed in Microcal Origin®. The data were fit to the following expression:

$$[HNO]_t = \frac{k_{eff}[H]_o}{k_w - k_{eff}}(e^{-k_{eff}t} - e^{-k_w t}) \qquad (2)$$

where $k_{eff} = k_1[NO][M]$ (M = He), and $[H]_o$ is the initial concentration of atomic hydrogen in the flow tube in the absence of nitric oxide. The initial concentration of atomic hydrogen was not explicitly determined. The input value for $[H]_o$ was assumed to be approximately equal to $[HNO]_{z\,max}$ where z is the distance between the injector and the ICLAS axis of detection. When z was maximized, neither an increase in background pressure nor an increase in the concentration of NO yielded a higher concentration of HNO. Both of these indicators confirm that $[HNO]_{maximum} \approx [HNO]_{z\,max}$. It was also assumed that all the [HNO] formed at z_{max} was from the titration of atomic hydrogen with nitric oxide. This assumption leads to $[HNO]_{max} \approx [H]_o$. The number densities calculated for [HNO] are in good agreement with expected values: the concentration of atomic hydrogen generated from the discharge was estimated between 10^9-10^{10} molecules cm^{-3} and the calculated number densities for $[HNO]_{max}$ vary between 3 - 5 x 10^9 molecules cm^{-3}.

Considering potential systematic errors in the measurement of gas flows, pressure, and detector signal, as well as uncertainties associated with the Franck-Condon factors used to calculate the HNO number density, it is estimated that the rate constant can be determined with an accuracy of ±20%.

The termolecular rate constant reported in Table 1 is (4.3 ± 0.4) x 10^{-32} cm^6 $molecule^{-2}s^{-1}$. Clyne and Thrush[8] and Miyazaki and Takahashi[9] have determined the value of k_1 by measuring the decrease in HNO emission intensity in a discharge-flow system. They report values of (1.8 ± 0.3) x 10^{-32} cm^6 $molecule^{-2}$ s^{-1} and 3.0 x 10^{-32} cm^6 $molecule^{-2}$ s^{-1}, respectively. These are the only two values in the literature that report the formation of HNO with helium as a carrier gas. The work of

---

[8] M.A.A. Clyne and B.A. Thrush, *Disc. Faraday Soc.* 33, 139 (1962).
[9] S. Miyazaki and S. Takahashi, *Mem. Def. Acad. Japan* 9, 643 (1969).

Miyazaki and Takahashi[9] requires a complicated data reduction scheme, making a comparison of values extremely difficult.

Table 1: Observed termolecular rate constants at 13.85 and 24.00 Torr for the reaction, $H + NO \xrightarrow{M} HNO$

Pressure torr	velocity $10^3\ cm\ s^{-1}$	$[H]_o$ $10^9\ cm^{-3}$	$k_1 \pm \sigma$ $10^{-32}\ cm^6\ s^{-1}$	$k_{wall} \pm \sigma$ s^{-1}
13.85	5.3	4.15	3.0 ± 0.3	0.6 ± 0.3
	4.9	4.01	4.1 ± 0.4	0.5 ± 0.4
24.00	5.1	3.86	5.7 ± 0.4	0.7 ± 0.2
	5.1	3.92	4.7 ± 0.5	0.7 ± 0.4
	5.2	4.01	4.1 ± 0.4	0.5 ± 0.5

Although similar concentrations of nitric oxide were used in all experiments, the concentration of atomic hydrogen in the previous work was approximately 0.5-2% of the total flow. In this work, the concentration of atomic hydrogen was reduced to approximately 1×10^{-4} % of the total flow. Minimizing the concentration of atomic hydrogen limits the potential for other formation or recombination reactions involving atomic hydrogen. Similarly, limiting the concentration of atomic hydrogen limits the formation of HNO. This prevents potential losses of HNO via wall loss, self-reaction, or other successive reactions.

In the KICAS flow tube, the absorption spectrum of HNO is not observed if the nitric oxide stream is not purified by means of the LN2/pentane cold bath. Nitrogen dioxide exists as an impurity in the stream of NO from the cylinder. Nitrogen dioxide reacts much faster with atomic hydrogen than nitric oxide does. A rigorous purification of the NO stream is essential to measuring the rate parameters of (R1) and (R4) accurately. Clyne and Thrush[8] make a similar observation in that they are unable to detect the 'glow intensity' due to the emission of HNO at increased concentrations of nitrogen dioxide.

The work of Clyne and Thrush[8] neglects to account for any potential wall loss – for both HNO and atomic hydrogen. In our system, it is possible that the wall is acting as a third body and contributing to the stabilization of the electronically excited HNO^* molecule, as well as acting as a loss site. Similar recombination phenomena are possible with atomic hydrogen. The only indication of sensitivity to detecting HNO in the literature is given by observations associated with the steady-state concentration of HNO being much less than 0.2 [NO]. A rough estimate of the detection sensitivity reveals that the HNO was observed in concentrations around 10^{12}-10^{13} molecules cm^{-3}, much higher than the concentrations reported here. In the present work, we effectively reduced the concentration of HNO so that we could isolate the formation of HNO, followed by a slow wall reaction. At higher concentrations of HNO, it is unlikely that the slow self-reaction,

$$HNO + HNO \rightarrow H_2O + N_2O \qquad (R5),$$
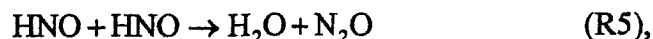
becomes significant; however, it is likely that higher concentrations of HNO will affect the fast reaction,

$$HNO + H \rightarrow H_2 + NO \qquad\qquad (R3).$$

Although (R3) is and should be considered in the study by Clyne and Thrush[8], the potential of this reaction to skew the measured concentration of HNO in the ICLAS system is minimized by manipulating the number densities and flows such that [NO]>>[H], [HNO].

The total pressure in the system employed by Clyne and Thrush[8] was 5-10 times lower than the pressures used in this experiment. Under the experimental conditions reported by Clyne and Thrush, it is interesting to note that $k_3 > k_2[M]$. This is not the case in our experiment. By limiting the concentration of atomic hydrogen and the formation of HNO, we were able to observe a steady-state concentration of HNO (at about 6 msec of reaction time).

The wall loss reaction is reported with high uncertainties because of the relatively small effect it has on the simulated curve up to a value of $1\ s^{-1}$. The upper limit for the rate constant of the wall reaction for this system is reported as $1\ s^{-1}$, and is most likely in the range $0.2\text{-}0.7\ s^{-1}$, which is in good agreement with other reported values. At values above $1\ s^{-1}$, the curve fitting function, eq (2), begins to demonstrate behavior inconsistent with the experimental observations. On the time scale of the experiment ($\sim$20 msec), a value greater than $1\ s^{-1}$ would demonstrate a slow, but detectable decline in the concentration of HNO. All of the experimental data at varying pressures observed here supports a slower decay associated with the wall reaction.

The Aurora application, part of the CHEMKIN® software package, simulates the time evolution or steady state of a well mixed reactor. The Aurora application was used to model the series of reactions ((R1) – (R4)) in the HNO reaction system in order to compare numerically modeled kinetics curves with the experimental curves obtained from the KICAS measurements. The rates used in the simulations were: $k_1 = 4.3 \times 10^{-32}\ cm^6\ molecule^{-2}\ s^{-1}$, $k_2 = 6 \times 10^{-33}\ cm^6\ molecule^{-2}\ s^{-1}$, $k_3 = 1.7 \times 10^{-12}\ cm^3 molecule^{-1}$ and $k_w = 0.5\ s^{-1}$. The application was run under conditions appropriate to the experiments reported above. The simulated kinetics curves showed good agreement with the experimental data[10].

Conclusion. – ICLAS has been demonstrated as a feasible detection method for trace species in a discharge flow tube. This implementation has been used to measure the rate of the reaction between atomic hydrogen and NO to form HNO in helium carrier gas. A reaction rate constant of $(4.3 \pm 0.4) \times 10^{-32}\ cm^6\ molecule^{-2}\ s^{-1}$ at 295 K was measured for the reaction H + NO + M $\rightarrow$ HNO + M (M = He). The pressure and concentration range enabled by ICLAS detection has allowed us to limit reactive pathways that would inhibit the formation of HNO. The sensitivity of ICLAS, coupled with the versatility of the discharge flow technique, suggests that intracavity absorption spectroscopy will be a useful technique for kinetics measurements on free radicals and other reactive species. These results have been published[11].

The KICAS method described here is essentially equivalent to similar methods used in kinetic studies employing Cavity Ring Down Spectroscopy in a pulsed-photolysis or discharge-flow configuration. The primary difference between KICAS and CRDS-based experiments is the accessible spectral range of the spectroscopic system employed. The SKaR (Simultaneous Kinetics and Ring-down) method recently reported by Brown et al.[4] represents an analogous method. The sensitivity of both SKaR and KICAS are comparable. One specific advantage that KICAS or a conventional configuration for CRDS detection may have over SKaR is the time scale accessible for kinetic measurements, as SKaR is inherently limited by the empty cavity time

[10] P. Sheehy, Ph.D. Thesis, Massachusetts Institute of Technology (May 2005).

[11] P. Sheehy and J.I. Steinfeld, *J. Phys. Chem.* **109**, 8358 (2005).

constant (τ_0) which the authors state is variable up to hundreds of microseconds. To be a candidate for SKaR, a reaction must have kinetics on the order of τ_0. The experiment reported here was carried out at time scales up to 20 msec, well beyond the range of SKaR. On the other hand, SKaR is an attractive option for kinetics experiments at short time scales, as a laser light pulse into the cavity initiates the experiment and controls the timescale, whereas KICAS requires a more complicated discharge flow configuration to operate at shorter time scales. Both methodologies have their merit, and should be considered complementary.

2.   Extending the Spectral Range of ICLAS for Detecting the Hydroperoxyl Radical (HO$_2$)

The hydroperoxyl radical, HO$_2$, is an important intermediate in both atmospheric and combustion chemistry. The spectroscopy of the radical has been studied extensively with the hope of developing sensitive methods for detecting trace levels of HO$_2$ in the atmosphere and in laboratory experiments. The near-infrared spectrum of HO$_2$ has been studied in emission spectroscopy, but not as much via absorption techniques; few high resolution studies exist of its near-infrared absorption spectrum. HO$_2$ transitions in the near-IR are difficult to measure via absorption techniques because of its weak oscillator strength ($\sigma \cong 10^{-21}$ cm^2 molecule^{-1}) and because of the spectral region in which it is located.

Fink and Ramsay observed that the 000 – 000 and 001 – 000 bands of the $A\ ^2A' \leftarrow X\ ^2A''$ transitions at 1.43 μm and 1.26 μm, respectively, fall into "atmospheric windows" and that long-pass absorption measurements were possible with InGaAsP or InGaAs diode lasers. Although both of these transitions are slightly outside the range of our ICLAS system, this observation regarding absorption measurements using multi-pass techniques can be applied to the 003 – 000 and 004 – 000 transitions in the near infrared. The spectral range of our ICLAS system is limited by the lasing medium, Ti:sapphire, and the silicon diode array detector. Neither the Ti:sapphire crystal nor the diode array detector are capable of operating beyond 1.1 μm. The 003 – 000 and 004 – 000 transitions are at 1.024 μm and 0.945 μm, respectively. Both regions would be accessible using ICLAS with additional tuning elements, as described below. Optimistically, an ICLAS experiment could be designed to detect the 004 – 000 bands at 0.945 μm; however, a strong absorption band of water in this same region precludes any static measurements on this band.

Based on Fink and Ramsay's detection of the 000 – 000 and 001 – 000 bands of the $A\ ^2A' \leftarrow X\ ^2A''$ electronic transition, the absorption cross section of the 003 – 000 transition is estimated to be 4 x 10^{-21} cm^2 molecule^{-1}. With an occupation ratio of 50% and a generation time of 1 ms, it should be possible to achieve an effective path length of 1.5 x 10^7 cm (150 km), which would yield an absorbance in the range of 5% to 60%. If detection of the HO$_2$ radical can be achieved using ICLAS, it would be worthwhile to attempt to conduct kinetic measurements to reduce the uncertainties in reported rate coefficients. It may be possible to clarify reaction pathways in the presence of water vapor and, depending on the spectral features and resolution, detect the proposed water-radical complex.

Experimental Approach. – An ICLAS edge-tuner was employed to extend the tuning range to wavelengths longer than 1000 nm. Operation of the laser at the edge of its gain curve requires a strong frequency selector, with the selector loss rapidly increasing on the shorter wavelength side. An edge tuner meeting these requirements was designed and installed by Dr. A Kachanov in

9

March 2005. The idea of this tuner is to use the rather strong spectral dependence of the short-wavelength edge of a multi-layer dielectric mirror for S-polarization. A pair of parallel mirrors is inserted in front of the output coupler of the Ti:sapphire laser. This pair is mounted on a rotation stage with the center of the tuning mirror TM1 coincident with the axis of rotation of the stage. (See Figure 5, following page). The angle of incidence on the mirror TM1 is large ($\cong 70°$). The reflection for S-polarization is high until about 1000 nm when it starts dropping rapidly. Such situation would occur if the mirror TM1 were initially designed for a central wavelength of about 1400 nm. The mirror TM2 serves only as a high reflector at the wavelength of 1000 nm, and it should have flat reflectivity curve around this wavelength which should spread equally to the both sides of this wavelength. Such a property can be achieved for the design wavelength of about 1170 nm.

To confirm the tuning of the ICLAS laser beyond 1000 nm, an asymmetrically Z-folded standing wave, linear cavity configuration was used. The output of the 15-W argon ion laser pumped the Ti:sapphire laser situated between two spherical folding mirrors with a radius of curvature of 15 cm. The edge tuner was placed between the sample cell and the output coupler. The first mirror in the edge tuner (TM1) was used at the short wavelength edge of its reflectivity curve. The second mirror was greater than 99% reflective for the wavelength region 940 – 1140 nm. The output coupler had a diameter of 1.5 cm, with a 3 degree wedged substrate, and had a reflectivity of 99%. The tuning of the laser from 960 to 1040 nm was confirmed using a diffraction grating and the output of the argon ion laser that is coupled with the Ti:sapphire laser. Broadband lasing of the Ti:sapphire was observed, between the 7th and 9th orders of diffraction of the argon ion laser of 514.5 nm, near the 8th order of diffraction at 1029 nm.

Although the extension of the spectral range of the ICLAS instrument with the edge tuner was only 40 nm, this provides a significant benefit since it should make possible the detection of the 003 – 000 band of the $A\,^2A' \leftarrow X\,^2A''$ electronic transition of HO_2. Future applications of the ICLAS and KICAS techniques could exploit this capability to provide new information about this important atmospheric radical species.

Figure 5. Edge tuner configurations and reflectance curves (data provided by Dr. A. Kachanov, Picarro Inc., Sunnyvale, California, March 2005).
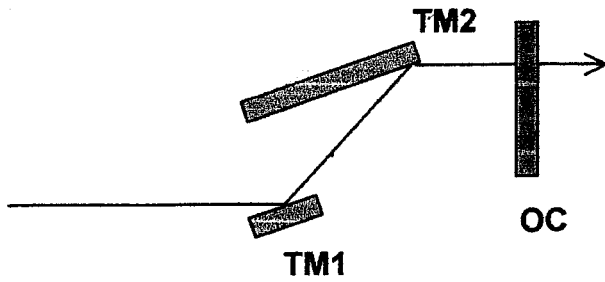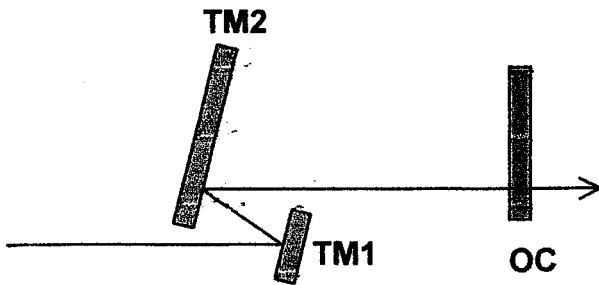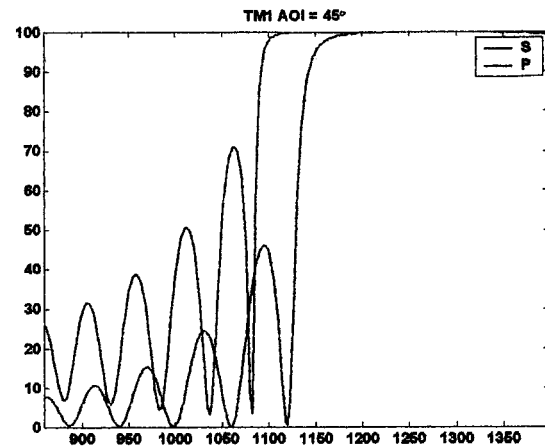

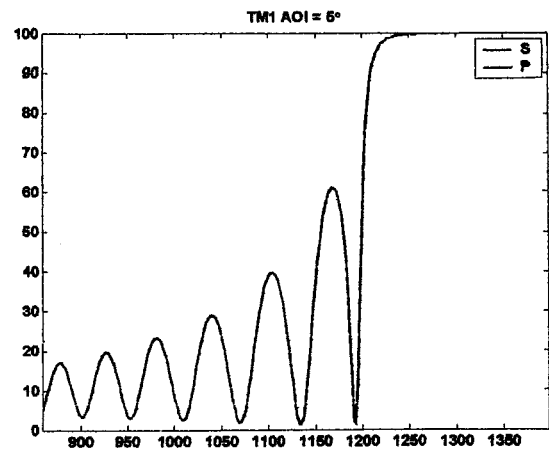**1. large AOI (~70°)**

Operating at 1000 nm on S-polarization
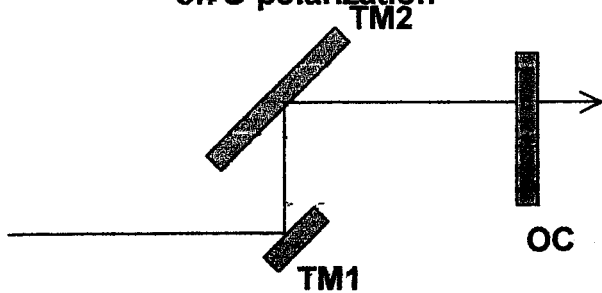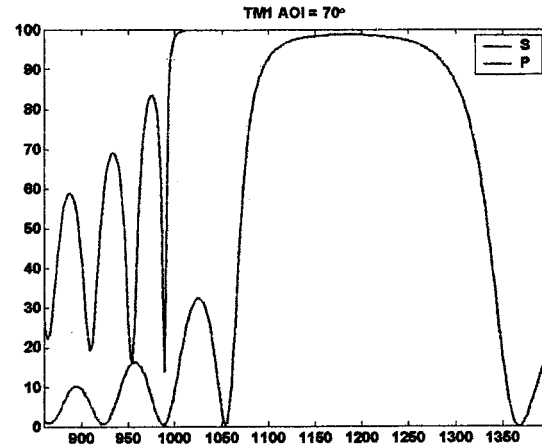
2. medium AOI (~45°)

Operating at 1120 nm on S-polarization

3. small AOI (~ 5°)

Operating at 1230 nm on S-polarization

3. Modeling OH and HO$_2$ in the Mexico City Metropolitan Area (MCMA)

The hydroxyl radical, OH, and the hydroperoxyl radical, HO$_2$, play significant roles in many chemical processes in the atmosphere, including ozone formation, aerosol formation, and acid rain. Photochemically generated radicals – HOx (OH and HO$_2$) and ROx (HO$_2$ + RO$_2$) – are a major part of understanding tropospheric chemistry. The OH radical is the atmosphere's most important oxidizing species, while the HO$_2$ radical is a major reactive component in the process that leads to the formation of tropospheric ozone. Studying the processes of both radicals is essential to understanding the general oxidative capacity of the atmosphere. Because these radicals initiate and participate in an overwhelming majority of the atmosphere's chemical pathways, it is essential that we understand the factors that influence their production, recycling, and removal.

In collaboration with the atmospheric modeling group of Prof. Mario Molina's MCMA Project[12], a kinetic box model for the MCMA urban troposphere was successfully constructed and employed to explore HOx and VOC chemistry. Three cases were analyzed to highlight the performance of the box model in predicting HOx concentrations: no HOx constraints, constraints on HO$_2$ only, and constraints on OH only. The model performed reasonably well for all three cases during the daytime hours; however, discrepancies remained between observed and modeled values. Modeled values for HOx were consistently lower than those observed during the MCMA campaign, indicating that the radical budget – and the oxidative capacity – of the urban troposphere were not completely represented by the box model. This notion of missing reactivity has been observed in chamber experiments and confirmed in field studies. The more significant underestimation of the modeled values during the night-time hours suggests that night-time sinks are too strong or, more likely, that there is a night-time source of HOx that is not included in the model. For example, biogenic compounds can contribute to peroxy radicals at night due to ozonolysis and reaction with NO$_3$ radicals.

The box model was used to confirm the prediction of Volkamer et al. that the concentration of glyoxal, a new indicator for VOC oxidation, is overestimated by the model for two reasons: secondary formation of glyoxal from recycling processes and a lack of sink terms, particularly heterogeneous chemistry.

During the coming year, further validation of the oxidation scheme in the model will be carried out by the former graduate student associated with the NASA grant (now a postdoctoral research associate in the Molina group) by a combination of modeling and field measurements in the MCMA. One of the principal issues to be explored is the ability of the model to predict the concentrations of oxidation products such as glyoxal, cresol, and phenol, each of which had been measured during the 2003 MCMA field campaign.

Publications and Presentations (Cumulative)

1. J.I. Steinfeld and R.R. Gamache, "Energy Transfer and inelastic collisions in ozone", *
   Spectrochim. Acta **A54**, 65 – 76 (1998).

---

[12] L.T. Molina and M.J. Molina, *Air Quality in the Mexico Megacity: An Integrated Assessment*, Kluwer Academic Publishers, Dordrecht, 2002.
* Received Harold W. Thompson Award for the most significant article published in *Spectrochimica Acta* during 1998.

2. I. Dubinsky, K. Rybak, J.I. Steinfeld, and R.W. Field, "Frequency-Modulation-Enhanced Remote Sensing", *Appl. Physics* **B67**, 481 – 492 (1998).

3. S.K. Witonsky, M. Canagaratna, S. Yang, S.L. Coy, R.W. Field, and J.I. Steinfeld, "Measurements on Water Vapor and other Atmospheric Absorbers using Intracavity Laser Absorption Spectroscopy", Proceedings, International Conference on Water in the Gas Phase (Université Marne-la-Vallée, France, June 1998), p. 106.

4. J.I. Steinfeld, M. Gardner, M. Canagaratna, S. Yang, B. Gibbs, S. Witonsky, and T. Raine, "Spectroscopic Database Requirements for Air Quality Monitoring and Regulation", Proceedings, HITRAN Database Conference (Hanscom AFB, Bedford, Mass., Sept. 1998), p. 21.

5. S. Tai, S. Papasavva, J.E. Kenny, B.D. Gilbert, J.A. Janni, J.I. Steinfeld, J. Taylor, and R. Weinstein, "Reassignment of the vibrational spectra of CH_3CHF_2 (HFC-152a), CH_3CF_3 (HFC- 143a), CHF_2CF_3 (HFC-125), and $CHCl_2CF_3$ (HCFC-123)", *Spectrochim. Acta* **55A**, 9 – 24 (1999).

6. J.I. Steinfeld, "New Spectroscopic Methods for Environmental Measurement and Monitoring", *Chinese J. Chem.* **17**, 204 (1999).

7. S.F. Yang, M. Canagaratna, S. Witonsky, S. Coy, J.I. Steinfeld, and R.W. Field, "Intensity Measurements and Collision-Broadening Coefficients for the Oxygen A-band measured by IntraCavity Laser Absorption Spectroscopy", *J. Mol. Spectroscopy* **201**, 188 – 197 (2000).

8. J.I. Steinfeld, R.W. Field, M. Gardner, M. Canagaratna, S.F. Yang, A. Gonzalez-Casielles, S. Witonsky, P. Bhatia, B. Gibbs, B. Wilkie, S.L. Coy, and A. Kachanov, "New Spectroscopic Methods for Environmental Measurement and Monitoring" (SPIE Symposium Proceedings on *Environmental and Industrial Sensing: Environmental Monitoring and Remediation Technologies*, Boston, Mass., Sept. 1999).

9. S.K. Witonsky, M.R. Canagaratna, S.L. Coy, J.I. Steinfeld, R.W. Field, and A.A. Kachanov, "The $3v_1$ overtone band of HONO: Rovibrational Parameters and Band Intensity using IntraCavity Laser Absorption Spectroscopy", presented at International Symposium on Molecular Spectroscopy (Columbus, Ohio, June 2000).

10. S.K. Witonsky, M.R. Canagaratna, S.L. Coy, J.I. Steinfeld, R.W. Field, and A.A. Kachanov, "The $3v_1$ overtone band of *trans*-nitrous acid: Rotational and perturbation analysis and absolute intensity", *J. Chem. Phys.* **115**, 3134 – 3143 (2001).

11. P.M. Sheehy, S.K. Witonsky, and J.I. Steinfeld, "Improvements in spectroscopic and kinetic parameters by IntraCavity Laser Absorption Spectroscopy (ICLAS)", presented at Workshop on Laboratory Spectroscopic Needs for Atmospheric Sensing (San Diego, Calif., October 2001).

12. J.I. Steinfeld, P. Sheehy, and S. Witonsky, "Sampling and Analysis of Components of the Terrestrial Atmosphere", presented at Symposium on Environmental Sampling and Analysis, American Chemical Society National Meeting (Boston, Mass., August 2002).

13. P. Sheehy and J.I. Steinfeld, "Discharge-Flow Kinetics Measurements using IntraCavity Laser Absorption Spectroscopy", *J. Phys. Chem. B* **109**, 8358 – 8362 (2005).

14. P. Sheehy, "Laboratory Measurements and Modeling of Trace Atmospheric Species", Ph.D. Thesis, Massachusetts Institute of Technology (May 2005).